Geometry of twist transport in a rotating elastic rod

Hirofumi Wada
Yukawa Institute for Theoretical Physics, Kyoto University, Sakyo, 606-8502 Kyoto, Japan
(Received 22 February 2011; published 13 October 2011)

An elastic rod rotating in a viscous fluid undergoes a shape transition from a twirling (axial spinning) to a whirling state (crankshafting motion) at a certain critical frequency [Wolgemuth *et al.*, Phys. Rev. Lett. **84**, 1623 (2000)]. The physical properties of such whirling rods are largely unknown, owing to their strongly nonlinear character. We analytically and numerically demonstrate that this dynamical transition occurs to reduce the viscous energy dissipation. A simple geometric interpretation underlying this observation is also given. These results provide a fundamental scenario for viscous twist transport in flexible filaments and are potentially important in the analysis of biopolymer dynamics such as DNA supercoiling during transcriptions.

DOI: 10.1103/PhysRevE.84.042901 PACS number(s): 87.16.Ka, 05.45.−a, 46.70.Hg

I. INTRODUCTION

The buckling of a thin elastic rod subjected to an external load has a long history of study in mechanics, dating back to Euler and Kirchhoff [1,2]. The diverse forms of filaments and polymers found in biology have kept this classical subject a fascinating one in the fields of biological physics and applied mathematics [3]. The geometric and mechanical interplay in twisted filaments is of particular interest [4].

Unlike a self-avoiding closed curve where the linking number Lk, which is the sum of twist Tw and writhe Wr, is invariant under any deformation [5,6], the topological aspects of open curves are often more involved. The concept of writhe has been previously generalized to open curves, and its nontrivial role in DNA twist elasticity has also been recognized in relation to geometric phases [7–9]. It is mentioned that an open polymer can release its axial rotation of 4π by rotating around its end once [7,8]. Geometrically, this refers to the well-known importance of the spinor representation of the rotation group [8,10,11]. However, the role of this writhing geometry in the *driven dynamics* of elastic filaments [12] appears to have been much less explored so far, which is the purpose of the present study.

Specifically, we study an isotropic elastic rod that is axially rotated at one end at frequency ω_0 with the other end free (see Fig. 1). This model system exhibits a rich variety of elastohydrodynamic phenomena and was first proposed and analyzed by Wolgemuth *et al.* [13]. They showed that a shape instability occurs at a critical frequency ω_c. For $\omega_0 < \omega_c$, the rod remains straight and undergoes simple axial spinning (*twirling*), but for $\omega_0 > \omega_c$ the rod buckles and exhibits a combination of axial spinning and rigid-body rotation (*whirling*). Large-amplitude whirling in the stationary state was later demonstrated numerically [14,15]. However, a detailed physical understanding of whirling dynamics is still lacking because of its strongly nonlinear character. In this Brief Report, we calculate the nonlinear dependence of the energy dissipation rate on the driving frequency and demonstrate that dynamical buckling occurs to reduce the dissipation. We also show its simple geometric origin. Our results elucidate a previously unknown role of the writhing geometry in the energetics of the dynamical transition of forced filaments. This is conceptually important, since it may open up a new way to characterize the nature of *dynamic* buckling of a driven filament by analogy with the well-established energetic theory of its *static* buckling transition, where the elastic energy is minimized for a buckled configuration.

II. MODEL

We study the overdamped dynamics of an isotropic and inextensible rod of total length L and radius a. The force and moment balance of the rod can be described by the Kirchhoff rod equations [1,2]

$$\partial_s \mathbf{F} - \mathbf{f}_v = 0, \tag{1}$$

$$\partial_s \mathbf{M} + \hat{\mathbf{t}} \times \mathbf{F} - \mathbf{m}_v = 0, \tag{2}$$

where $\mathbf{r}(s,t)$ is the rod's centerline position parameterized by arc length s and $\mathbf{t} = \partial_s \mathbf{r}$ is the unit tangent vector. $\mathbf{F}(s)$ and $\mathbf{M}(s)$ are the internal force and moment acting on the rod cross section at s, and $-\mathbf{f}_v$ and $-\mathbf{m}_v$ are the viscous drag force and moment per unit length. Neglecting the anisotropy of friction coefficients for a slender rod due to hydrodynamic interactions, we assume $\mathbf{f}_v = \zeta \mathbf{v} = \zeta \dot{\mathbf{r}}$ and $\mathbf{m}_v = \zeta_r \omega \hat{\mathbf{t}}$, where ζ and ζ_r are translational and rotational friction coefficients proportional to fluid viscosity η, respectively [16]. The constitutive relation for an isotropic rod with bending and twisting moduli A and C is given by $\mathbf{M} = A\hat{\mathbf{t}} \times \partial_s \hat{\mathbf{t}} + C\Omega\hat{\mathbf{t}}$, where $\Omega(s)$ is the twist density [2]. The tangential component of Eq. (2) gives the viscous torque balance about the tangent:

$$\zeta_r \omega = \hat{\mathbf{t}} \cdot \partial_s \mathbf{M} = C \partial_s \Omega. \tag{3}$$

To express the dynamics in terms of $\mathbf{r}(s,t)$ and twist $\Omega(s,t)$, it is useful to employ the following geometric relation for twist density [13,17]:

$$\dot{\Omega} = \partial_s \omega - \Omega \hat{\mathbf{t}} \cdot \partial_s \dot{\mathbf{r}} + (\hat{\mathbf{t}} \times \partial_s \hat{\mathbf{t}}) \cdot \partial_s \dot{\mathbf{r}}. \tag{4}$$

This equation describes how twist is transported along the rod centerline; it is a local conservation law for Ω [13,17]. The first term on the right-hand side implies that twist changes if the axial rotational velocity is not uniform along the curve. This term describes the diffusive transport of twist, and thus $-\omega(s)$ is interpreted as the twist current. The second term is the stretch-twist coupling, which is absent in our inextensible rod. The third term accounts for the change in twist due to writhing (out-of-plane bending) [18]. This term is explicitly nonlinear and is usually interpreted as a sink or source in the

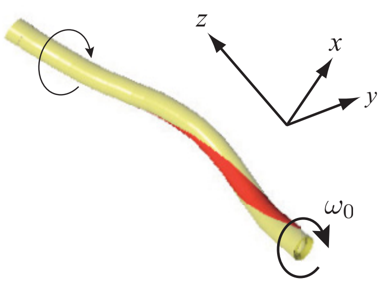

FIG. 1. (Color online) Schematic diagram of our model system. An isotropic elastic rod is forced to rotate at frequency ω_0 at its clamped base with the other end free in a viscous fluid of viscosity η.

twist dynamics. Substituting Eq. (3) into Eq. (4), we can obtain the dynamic equation for twist [13]. At the forced boundary, we impose $\mathbf{r}(0) = \mathbf{0}$, $\partial_s \mathbf{r}(0) = \hat{\mathbf{z}}$, and $\omega(s = 0) = \omega_0$, while at the free end the force and moment vanish, i.e., $\mathbf{F}(L) = \mathbf{0}$ and $\mathbf{M}(L) = \mathbf{0}$.

At low frequencies, the rod is twisted but remains straight along $\mathbf{z} = \hat{\mathbf{t}}(0)$, in which twist Ω obeys the diffusion equation $\dot{\Omega} = (C/\zeta_r)\partial^2\Omega/\partial s^2$. Noting the viscous torque balance at $z = 0$, i.e., $\zeta_r\omega_0 = C\partial_s\Omega(s = 0)$, Wolgemuth *et al.* [13] found that the steady-state twist profile is linear in space: $\Omega(s) = (\zeta_r\omega_0/C)(s - L)$. Therefore, the external torque M_{ext} that must be applied at the base to maintain a constant rate of rotation obeys $M_{\text{ext}} = -C\Omega(0) = \zeta_r\omega_0 L$, which is proportional to ω_0. The energy balance in the stationary state implies that the total energy dissipation rate P, i.e., the power expended by the motion of the rod, is equal to the work done externally on the rod per unit time. Thus, $P = \omega_0 M_{\text{ext}}$. This relation holds for all ω_0 as long as the system is stationary. In the case of twirling, we have

$$P = \zeta_r\omega_0^2 L. \tag{5}$$

Physically, a shape instability appears when the twisting external torque $M_{\text{ext}} = \zeta_r\omega_0 L$ becomes comparable to the bending torque A/L. An exact numerical analysis using linearized equations gave $\omega_c = 8.9A/(\zeta_r L^2)$ [13].

III. NONLINEAR DYNAMICS

Numerical approaches are necessary to study the nonlinear time evolution of the rod shape for $\omega_0 > \omega_c$. In our simulations, a rod is modeled as a chain of N spheres of radius a connected by sufficiently stiff springs that limits the change of contour length at a negligible level. The elastic energy is given in terms of the Euler angles that describe the transformation between consecutive tangent vectors in the chain. The elastic force and torque acting on each sphere are calculated using the variational method [19]. Neglecting inertia, the viscous force and torque balance equations are integrated by the explicit Euler method.

Upon buckling, the free end traces out a circle about the rotational axis, whose radius increases exponentially with time until the rod bends downward. The rod then reaches the stationary state and exhibits rigid-body-like motion, while spinning rapidly about its local tangent; see Fig. 2 [14,15]. The dynamics is more quantitatively characterized by plotting M_{ext} as a function of ω_0 during the transition (inset of Fig. 3). The numerical data at a low frequency confirm the predicted linear relation for twirling. Interestingly, however, the torque M_{ext} grows only sublinearly with ω_0 after the buckling. Thus, the whirling rod becomes easier to rotate for $\omega_0 > \omega_c$ compared with a twirling rod at the same ω_0. Correspondingly, the energy dissipation rate P increases more slowly than that expected from Eq. (5); see also Fig. 3.

This finding appears to be at odds with the expectation that the rod must consume a much larger viscous power to undergo crankshafting motion. The key to understanding this counterintuitive observation is the geometric relation for twist dynamics Eq. (4). Note first that the rod centerline exhibits the crankshafting motion with a frequency χ independent of time, i.e., $\dot{\mathbf{r}} = \chi\hat{\mathbf{z}} \times \mathbf{r}(s)$, where $\hat{\mathbf{z}} = \hat{\mathbf{t}}(0)$ is the axial spinning axis. Substituting this into Eq. (4) (with $\mathbf{t}\cdot\partial_s\dot{\mathbf{r}} = 0$), we obtain the local conservation law for twist *without* any source terms, $\dot{\Omega} + \partial_s j = 0$. The corresponding "effective" twist current density is given by

$$j(s) = -\omega(s) + \chi\cos\theta(s), \tag{6}$$

where we have defined $\hat{\mathbf{z}}\cdot\hat{\mathbf{t}}(s) = \cos\theta(s)$. In addition to the diffusive current $-\omega$, Eq. (6) has an additional contribution, $\chi\cos\theta$, which describes the change in twist due to writhing. Note, however, that it is not generally true that a twist current can be expressed in such a form as Eq. (6). As emphasized by Eq. (4), the twist current should be expressed as $-\omega$ and the writhing term generally acts as a source of Ω [13]. In our particular case, however, steady-state crankshafting motion exhibits an axial symmetry that allows us to define the twist current in the form of Eq. (6).

In the steady state, an injected twist at $s = 0$ has to exit the rod at $s = L$ in the form of either axial spinning or writhing,

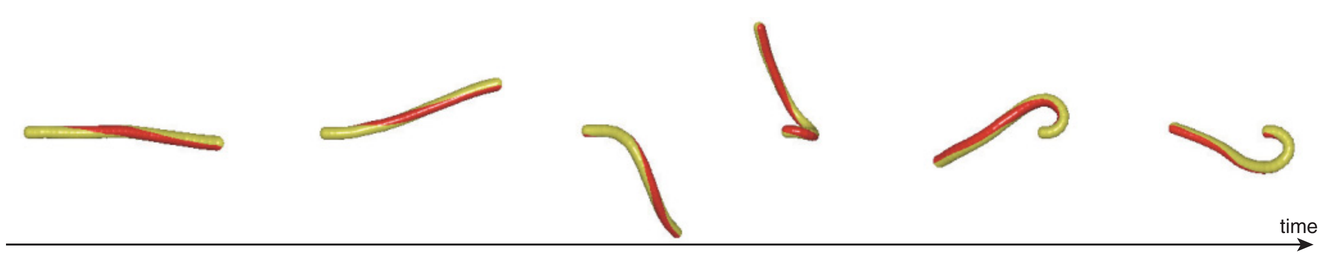

FIG. 2. (Color online) Trajectory of shape changes during the twirling-whirling transition. For $\omega_0 > \omega_c$, twirling (axial spinning) becomes unstable and the rod buckles to realize a large-amplitude whirling state. The snapshots here are obtained from our dynamic simulations for $L/a = 30$ and $\omega_0/\omega_c = 1.2$ [15,19].

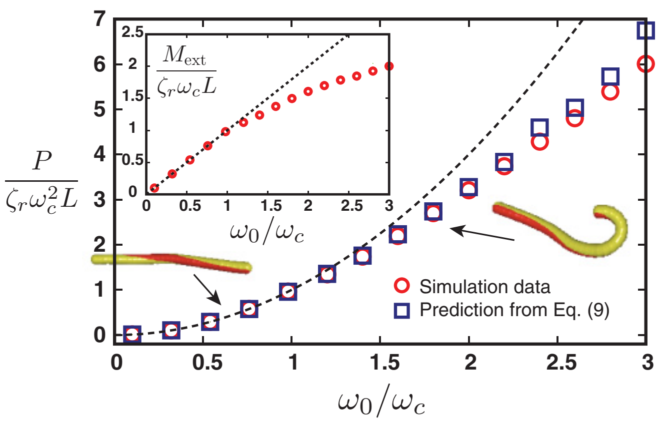

FIG. 3. (Color online) Relationship between dissipation rate P and frequency ω_0 obtained from our simulations and analytic argument. Red circles correspond to P "measured" directly as the work done at the base per time $\omega_0 M_{\rm ext}$, while blue squares correspond to the prediction obtained from Eq. (9). The broken line is the relation given by Eq. (5). Inset: external torque $M_{\rm ext}$ is plotted as a function of ω_0/ω_c for the same simulation data. The dotted line shows the linear relation $M_{\rm ext} = \zeta_r \omega_0 L$, valid for twirling.

meaning that the twist current is constant, $j(s) = j(0) = -\omega_0 + \chi$. This condition leads to the geometric relation

$$\omega_0 = \omega(s) + \chi[1 - \cos\theta(s)]. \tag{7}$$

At the free end $s = L$, we have $\omega_0 = \omega(L) + \chi[1 - \cos\theta(L)]$. Note that essentially the same relation was previously given but only in the weak bending limit [13]. One finds immediately that the twist transport via writhing is maximized for $\cos\theta(L) = -1$ at a given ω_0.

Our argument so far depends only on geometry and is essentially free of physics. Substituting Eq. (3) into Eq. (7) and integrating over s, we obtain

$$C\Omega(0) = -\zeta_r \omega_0 L + \zeta_r \chi L(1 - \sigma), \tag{8}$$

where we defined the fractional extension of the rod $\sigma = z(L)/L$. Note that $\sigma = 1$ for twirling, $\sigma < 0$ for whirling, and $\int_0^L ds(1 - \cos\theta) = L(1 - \sigma)$. Despite the linearity of the elastic constitutive relations and viscous dynamics, we have found the nonlinear dependence of $M_{\rm ext}$ on ω_0 due to the change in rod shape (Fig. 3) similar to that found in Ref. [20]. To analyze this more quantitatively, we return to the Kirchhoff equations (1) and (2). Integrating Eq. (2) over the rod length, we obtain $\mathbf{M}(0) + \int_0^L [\mathbf{r}(s) \times \zeta \mathbf{v}(s)]ds + \int_0^L \zeta_r \omega(s)\hat{\mathbf{t}} ds = 0$. Using $\mathbf{v} = \chi \hat{\mathbf{z}} \times \mathbf{r}$ for a whirling rod and $\mathbf{M}(0) = A\hat{\mathbf{z}} \times \partial_s^2 \mathbf{r}(0) + C\Omega(0)\hat{\mathbf{z}}$, we obtain $C\Omega(0) + \zeta\chi \int_0^L |\mathbf{r}_\perp(s)|^2 ds + \zeta_r \int_0^L \omega(s)\hat{\mathbf{t}} \cdot \hat{\mathbf{z}} ds = 0$, where $\mathbf{r}_\perp(s) = [x(s), y(s), 0]$, which describes the overall torque balance between the rod's internal torque and the drag torque. Substituting Eqs. (7) and (8) into this, we arrive at $\chi = \omega_0 \zeta_r (1 - \sigma)L / \int_0^L ds[\zeta_r(1 - \cos\theta)^2 + \zeta|\mathbf{r}_\perp|^2]$. Assuming a uniformly bent rod at $\omega \approx \omega_c$, we obtain from this formula $\chi \approx 30A/(\zeta L^4) \approx \omega_c (a/L)^2$, in agreement with the value given in Ref [13]. The difference in the numerical prefactors stems from our neglect of the helical nature of the buckled rod. Finally, the dissipation rate in steady-state whirling is

$$P(\omega_0) = P_0 \left[1 - \frac{L(1-\sigma)^2}{\int_0^L ds[(1 - \cos\theta)^2 + (\zeta/\zeta_r)|\mathbf{r}_\perp|^2]}\right], \tag{9}$$

where $P_0 = \zeta_r \omega_0^2 L$ is given by Eq. (5). The torque-frequency relationship is immediately obtained from $M_{\rm ext}(\omega_0) = P(\omega_0)/\omega_0$. Note that the second term in the large bracket in Eq. (9), the nonlinear writhe correction term, is always positive for $\omega_0 > \omega_c$ and is essentially independent of the viscosity, which indicates that it has a purely geometric origin. Therefore, one arrives at a physically important conclusion: the role of the whirling transition is to reduce the energy dissipation. This result reveals an energetic origin of the large-amplitude whirling transition. Equation (9), as well as the data in Fig. 3, constitutes the main result of this paper.

To obtain an exact value of P, we still have to determine the shape of the entire rod to evaluate the integral in Eq. (9). We compare in Fig. 3 our prediction obtained from Eq. (9) with the data obtained directly from the numerical simulations. In the comparison, the rod shape was extracted from the numerical simulations to evaluate the integral in Eq. (9). There is very good agreement, which further validates our physical argument. At higher ω_0, deviations become visible because the assumed axial symmetry is violated by secondary shape bifurcations.

IV. DISCUSSION

The buckled rod undergoes a cycle of global motion and returns to its original shape, during which the driving base undergoes a rotation of 4π about its axis. There is a simple

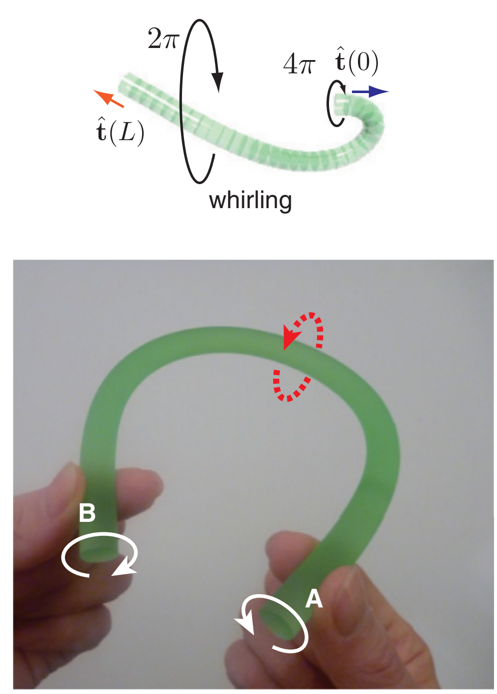

FIG. 4. (Color online) (Top) Geometric aspect of twist transport in a whirling rod: 2π global rotation removes the 4π axial twist. (Bottom) Simple demonstration with a rod bent into a half circle.

geometric interpretation for this observation; see Fig. 4. Take an open rod and fold it into a half circle. Upon the rotation of both ends by 2π in opposite directions, the rod executes a 2π rotation about its axis without changing its shape. Considering this phenomenon in a corotating frame at end A (shown in Fig. 4), the other end B executes a rotation of 4π about its tangent, while at the same time the rod centerline undergoes a global rotation of 2π about the tangent at A. This is expressed as $\omega_B - \omega_A = 2\chi$ on the basis of Eq. (7). Thus, the global whirling motion removes twist at the driving end twice as fast as axial spinning, with larger dissipation occurring as a tradeoff; see also Fig. 4 (top). This is why this mode prevails at elevated frequency ω_0. The geometric aspect of large-amplitude whirling is actually relevant to Feynman's plate trick, which shows the importance of the geometric phase when rotation and translation occur at the same time [10,11]. While this geometric argument is not mathematically new, it is helpful for more intuitively understanding why a rotating rod adopts such a distinct buckled shape.

V. SUMMARY

The twirling-whirling shape transition can be viewed as a means of decreasing the viscous dissipation. While our dynamics can be formulated in terms of the Rayleigh dissipation functional, the steady state of a rotationally driven rod cannot be understood by such a functional only and is distinct from the previous studies [21]. Although the present results were obtained by studying a specific system, our physical picture for twist transport in thin elastic media is robust and fundamental and potentially important for clarifying various biophysical phenomena, such as the looping and supercoiling dynamics of DNA driven by various DNA-processing proteins [22,23].

ACKNOWLEDGMENTS

Enlightening discussions with R. R. Netz and C. Schiller and financial support from the Ministry of Education, Culture, Sports, Science, and Technology of Japan (Grant in Aid, No. 22740274) are acknowledged.

[1] G. Kirchhoff, J. F. Math (Crelle) **50**, 285 (1859).

[2] A. E. H. Love, *A Treatise on the Mathematical Theory of Elasticity* (Dover, New York, 1944).

[3] F. B. Fuller, Proc. Natl. Acad. Sci. USA **68**, 815 (1971); I. Klapper and M. Tabor, J. Phys. A **27**, 4919 (1994); A. Goriely and M. Tabor, Phys. Rev. Lett. **80**, 1564 (1998); Nonlin. Dynam. **21**, 101 (2000); T. J. Healey, Math. Mech. Solids **7**, 405 (2002); A. Ghatak and L. Mahadevan, Phys. Rev. Lett. **95**, 057801 (2005); O. N. Yogurtcu, C. W. Wolgemuth, and S. X. Sun, Biophys. J. **99**, 3895 (2010).

[4] J. H. Michell, Messenger Math. **11**, 181 (1889); E. E. Zajac, ASME J. Appl. Mech. **29**, 136 (1962); A. Goriely, J. Elast. **84**, 281 (2006), and references therein; M. Wadati and H. Tsuru, Physica D **21**, 213 (1986); F. Tanaka and H. Tanahashi, J. Chem. Phys. **83**, 6017 (1986); J. F. Marko and E. D. Siggia, Phys. Rev. E **52**, 2912 (1995); G. H. M. van der Heijden and J. M. T. Thompson, Physica D **112**, 201 (1998); Nonlin. Dynam. **21**, 71 (2000); B. Fain, J. Rudnick, and S. Ostlund, Phys. Rev. E **55**, 7364 (1997); J. D. Moroz and P. Nelson, Proc. Nat. Acad. Sci. USA **94**, 14418 (1997); C. Bouchiat and M. Mezard, Phys. Rev. Lett. **80**, 1556 (1998).

[5] G. Calugareanu, Rev. Roum. Math. Pures Appl. **4**, 5 (1959); J. White, J. Am. Math. **91**, 963 (1969).

[6] F. B. Fuller, Proc. Natl. Acad. Sci. USA **75**, 3557 (1978).

[7] A. C. Maggs, J. Chem. Phys. **114**, 5888 (2001); V. Rossetto and A. C. Maggs, Eur. Phys. J. B **29**, 323 (2002); J. Chem. Phys. **118**, 9864 (2003).

[8] J. Samuel and S. Sinha, Phys. Rev. Lett. **90**, 098305 (2003); J. Stat. Phys. **143**, 399 (2011).

[9] S. Neukirch and E. L. Starostin, Phys. Rev. E **78**, 041912 (2008).

[10] R. P. Feynman, *Elementary Particles and the Laws of Physics: The 1986 Dirac Memorial Lectures* (Cambridge University Press, Cambridge, 1987).

[11] J. Samuel and R. Bhandari, Phys. Rev. Lett. **60**, 2339 (1988).

[12] R. E. Goldstein, T. R. Powers, and C. H. Wiggins, Phys. Rev. Lett. **80**, 5232 (1998).

[13] C. W. Wolgemuth, T. R. Powers, and R. E. Goldstein, Phys. Rev. Lett. **84**, 1623 (2000); T. R. Powers, Rev. Mod. Phys. **82**, 1607 (2010).

[14] S. Lim and C. S. Peskin, SIAM J. Sci. Comput. **25**, 2066 (2004).

[15] H. Wada and R. R. Netz, Europhys. Lett. **75**, 645 (2006).

[16] M. Doi and S. F. Edwards, *The Theory of Polymer Dynamics* (Oxford University Press, New York, 1986).

[17] R. D. Kamien, Eur. Phys. J. B **1**, 1 (1998); Rev. Mod. Phys. **74**, 953 (2002).

[18] J. Aldinger, I. Klapper, and M. Tabor, J. Knot Theory Ramifications **4**, 343 (1995).

[19] For more details of our simulation method, see Ref. [15] or G. Chirico and J. Langowski, Biopolymers **34**, 415 (1994); H. Wada and R. R. Netz, Phys. Rev. E **80**, 021921 (2009).

[20] S. A. Koehler and T. R. Powers, Phys. Rev. Lett. **85**, 4827 (2000); M. Manghi, X. Schlagberger, and R. R. Netz, *ibid.* **96**, 068101 (2006); B. Qian, T. R. Powers, and K. S. Breuer, *ibid.* **100**, 078101 (2008); N. Coq *et al.*, Phys. Fluids **20**, 051703 (2008).

[21] R. E. Goldstein, A. Goriely, G. Huber, and C. W. Wolgemuth, Phys. Rev. Lett. **84**, 1631 (2000).

[22] P. Nelson, Proc. Natl. Acad. Sci. USA **96**, 14342 (1999).

[23] H. Wada and R. R. Netz, Europhys. Lett. **87**, 38001 (2009).